CellPress

Review

More than Pictures: When MS Imaging Meets Histology

Yonghui Dong,[1] Bin Li,[2] and Asaph Aharoni[1,*]

Attaining high-resolution spatial information is a recurrent challenge in biological research, particularly in the case of small-molecule distribution. Mass spectrometry imaging (MSI) is an innovative molecular histology technique that could provide such information. It allows *in situ* and label-free measurement of both the abundance and distribution of a variety of molecules at the tissue or single cell level. The application of MSI in plant research has received considerable attention; thus, in this review, we describe the current state of MSI in plants. In particular, we present an overview of MSI approaches, highlight the recent technical and methodological developments, and discuss a range of applications contributing to the field of plant science.

Trends

Understanding the chemical complexity of plants requires novel technologies to track metabolites at the highest spatial resolution.

MSI is emerging as an advanced and essential molecular histology approach to map the distribution of plant molecules.

Recent technical and methodological advances in MSI technology have permitted its application in various fields of plant research.

Spatial Localization: The Missing Dimension in MS-Based Omics

The 'omics revolution', particularly for proteomics and metabolomics, is closely associated with technological development in MS. MS is currently the most efficient technology for molecule structural characterization, which has made significant inroads into providing a comprehensive understanding of biological functions [1]. Unfortunately, spatial information is frequently lost in MS-based holistic studies in which the analysis is performed on a tissue homogenate [2]. Significantly, higher plants comprise ten basic tissue types with approximately 15 structurally diverse cell types, which makes spatial analysis imperative [3]. The proteome and metabolome products measured within plants are all dynamic and spatial resolved [4]; therefore, knowing the spatial organization of the molecules at both the tissue and cellular levels will provide fundamental insights into plant biology [5].

A few techniques have been coupled off-line with MS to recover missing spatial information [6]. These techniques are typically based on the *in vitro* isolation and extraction of individual tissue and/or cell types, in which **fluorescence-activated cell sorting** (FACS) (see Glossary) and **laser-capture microdissection** (LCM) are the most prevalent tools [7]. Using such methodologies is operative in obtaining unique spatial information. However, they are typically time consuming and the molecules may undergo modification or degradation during sample preparation [8,9].

Mass Spectrometry Imaging in a Nutshell

MSI is an MS-based molecular histology technique that inherits from MS the unique advantages of high sensitivity, wide dynamic range, excellent molecular specificity, reasonable semiquantification capability, and the versatility to address many varied molecules in a single analysis [9]. The most distinctive advantages of MSI over other imaging techniques are its wide chemical identification capability and no requirement for detailed prior knowledge of the sample composition [10].

The basis of MSI is the **mass spectrometer**, which has three major parts: ion source, mass analyzer, and detector. In a prototypical MS experiment, the sample is delivered into the mass spectrometer, ionized, and vaporized in the ion source, and the resultant ions are sorted according to their mass:charge ratio (*m/z*) in the mass analyzer. Ions are finally detected in

[1]Department of Plant and Environmental Sciences, Weizmann Institute of Science, Rehovot, Israel
[2]Department of Chemistry and Beckman Institute for Advanced Science and Technology, University of Illinois at Urbana-Champaign, Urbana, IL, USA

*Correspondence: asaph.aharoni@weizmann.ac.il (A. Aharoni).

 http://dx.doi.org/10.1016/j.tplants.2016.04.007

the detector, and a plot of ion abundance against *m/z* represents a 'mass spectrum' [11]. Two acquisition modes are used in MSI, microprobe and microscope (Figure 1), which differ significantly in how the spatial information is obtained [12]. In the microprobe mode, a focused laser (e.g., matrix-assisted laser desorption ionization; MALDI) or primary ion beam (secondary

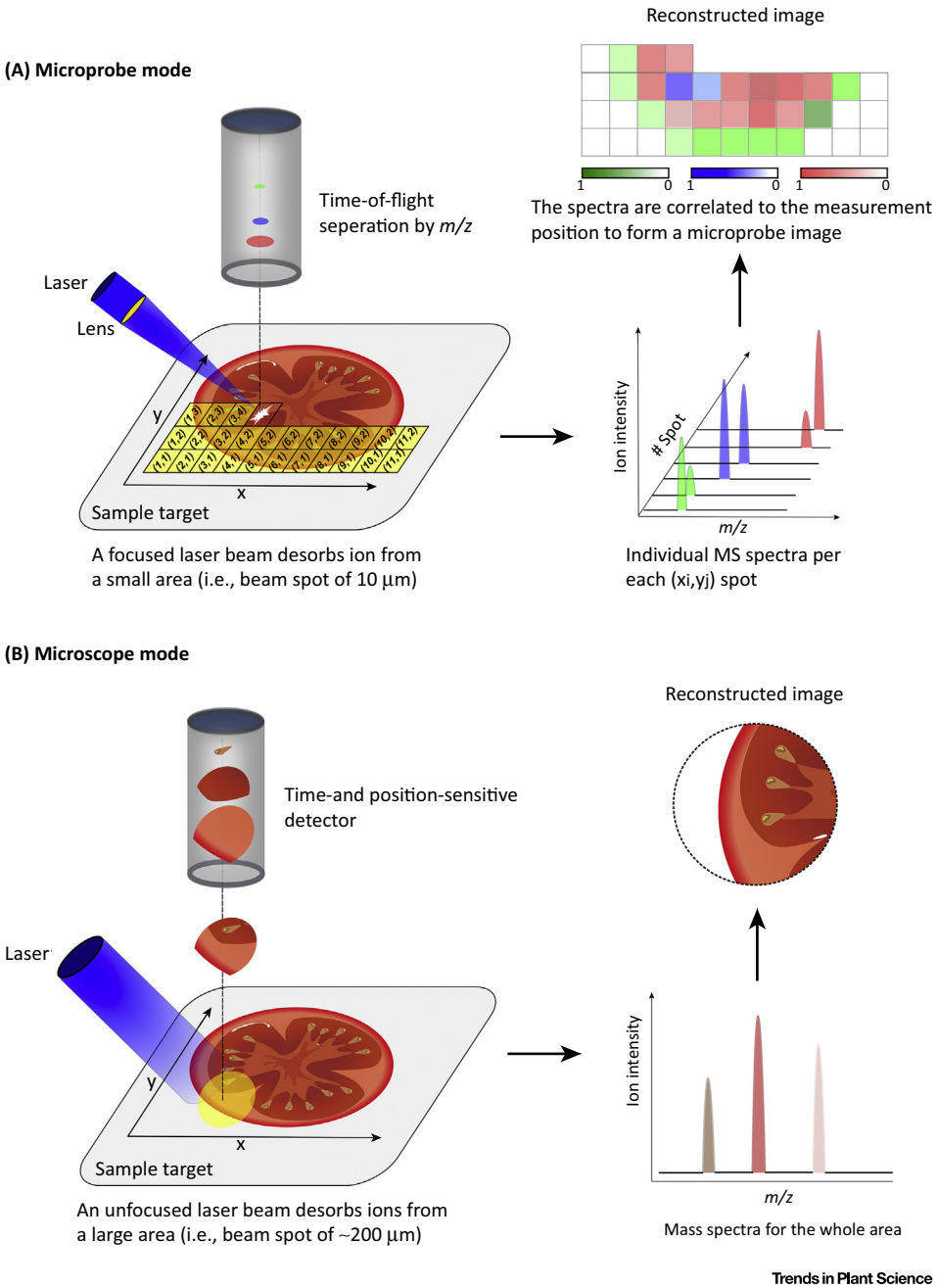

Figure 1. Schematic Overview of Microprobe and Microscope Mode Mass Spectrometry Imaging (MSI) Demonstrated on a Matrix-Assisted Laser Desorption Ionization (MALDI)-time-of-flight (TOF)/MS Platform. (A) In the microprobe mode MSI, a focused laser beam rasters the sample surface according to a predefined *x*, *y* grid. At each discrete spot, a mass spectrum is generated. An image with a pixel resolution equivalent to the beam size is reconstructed after the experiment. (B) In the microscope mode MSI, a broadly focused laser scans wide areas of the sample surface. Ion optics magnifies the molecular images and retains the spatial information. The molecular ion distributions are mapped on a position-sensitive detector.

Glossary

Depth resolution: a spatial resolution parameter used in 3D MSI. In the serial section-based 3D MSI, it refers to the tissue section thickness. In depth profiling-based 3D MSI, it refers to the profiling depth.

Fluorescence-activated cell sorting (FACS): a separation technique that enables a pool of different cells to be sorted one by one into one or more containers. The cells are typically sorted according to their specific light scattering and fluorescent characteristics.

Ion-mobility spectrometry (IMS): an analytical technique that separates gas-phase ions based on their size (*m/z*) and shape, analogous to electrophoresis in the condensed phase.

Laser-capture microdissection (LCM): an isolation technique that combines microscopy with laser beam technology, allowing for the isolation of target cells or tissue regions that need to be separated from others.

Mass:charge ratio (*m/z*): a value used in mass spectrometry obtained by dividing the mass of an ion by its charge number. For example, if an ion has a mass of 100 and a charge number of 1, its *m/z* is 100. An ion with a mass of 200 and a charge number of 2 also has an *m/z* of 100.

Mass spectrometer: an analytical instrument capable of ionizing analytes, separating them based on their *m/z*, and detecting them to produce a mass spectrum.

Reactive MSI: an MSI analysis approach where a compound that is capable of selectively reacting with analyte of interest is added into MSI (e.g., in the MALDI matrix or DESI spray solvent), allowing one to monitor the product of the reaction. This is usually carried out to increase the ionization yield of the target analyte or to isolate a specific isomer from a family of compounds.

ion MS; SIMS) is used to raster the sample tissue. At each spot, a full mass spectrum is generated. As a result, it becomes feasible to select an analyte signal from the array of mass spectra and plot the ion intensity for each spot across the tissue sample and, thus, visualize the distribution of individual molecular ions [12] (Figure 1A). Microprobe MSI is by far the most common approach, and its spatial resolution is largely defined by the size of the ionization beam [13]. By contrast, microscope MSI is still in an experimental phase [14]; in this mode, the laser or primary ion beam is defocused to irradiate a large sample area, typically 200 μm in diameter. The original position of the resulting ion cloud is maintained after ionization. A position-sensitive detection system is able to record both the ion intensity and the position of the ion impacting the detector surface, forming an ion-optical image [10,15] (Figure 1B). The spatial resolution of microscope MSI can reach 4 μm or less, which depends on the quality of the ion optics and detector resolution rather than on the size of laser focus or primary ion beam.

Several ion sources are available for MSI, among which SIMS, MALDI, and desorption electrospray ionization (DESI) are the most widely used [16,17]. Many other MSI sources are constantly being developed, mostly the derivatives or modifications of the above-mentioned ionization techniques. They differ in their methods of ion generation, pressure regime, spatial resolution, probing depth, and scope of application [14] (Table 1). For more detailed information, readers are kindly referred to many up-to-date reviews on this topic [14,18–22].

Although different MSI approaches require diverse workflows, they do share the major components in sample preparation, data acquisition, data preprocessing, image construction, and statistical analysis. Even though MSI techniques require limited sample preparation, it is the most crucial step for successful MSI analysis. Sample preparation should be carefully optimized according to the nature of the sample and analytes of interest to maintain the original localization and avoid analyte modification or degradation [4,18,23]. Sampling plant tissues is more challenging compared with mammalian tissues; for example, the surface cuticle and cell wall prevent direct MSI of internal analytes and plant tissues are more fragile upon freezing. It is also more difficult to get thin and intact sections for water-rich plant samples [23]. Specific issues associated with sampling plant tissues for MSI have been discussed in a recent review dedicated to this topic [23]. Given that MALDI imaging is the most widely used approach, a typical MALDI imaging pipeline is described in Box 1 to illustrate the MSI workflow.

Table 1. Overview of Various Ion Sources Used for MSI Analysis of Plant Samples[a]

Ion Source	Scanning Beam	Pressure Regime	Spatial Resolution	Application
SIMS	Primary ion beam	Vacuum	0.1–1 μm	Elements, atomic clusters and low molecular-mass compounds; depth profiling
LDI	UV laser	Vacuum, IP or AP	10–100 μm	Monitoring of molecular species containing a chromophore
MALDI	UV or IR laser	Vacuum, IP or AP	1–100 μm	Small molecules, lipid, peptides and proteins
LA-ICP	UV laser	AP	1–10 μm	Elements, especially metal ions; depth profiling
LAESI	IR laser	AP	100–300 μm	Small and large molecules; depth profiling
DESI	Charged spray-jet	AP	~200 μm	Small molecules, lipids and proteins
Nano-DESI	Liquid bridge	AP	10–100 μm	Small molecules, lipids and proteins

[a]Abbreviations: AP, atmospheric pressure; IP, intermediate pressure.

Box 1. Mass Spectrometry Imaging Workflow Demonstrated with MALDI Imaging

Plant tissues are first snap-frozen and sectioned with a typical thickness of 10–50 μm on a cryostat without using any embedding or fixing agents [19]. Dedicated samples (e.g., tomato fruit) may be embedded in a MSI-compatible medium, such as gelatin or carboxymethyl cellulose (CMC) solution. Once sliced, sample sections are thaw-mounted on glass slides or other MS-compatible holders, and vacuum dried in a desiccator. To promote desorption and ionization, a chemical matrix can be applied with 'wet' (e.g., spraying) or 'dry' (e.g., sublimation) coating methods, with the objective of obtaining a homogeneous layer of fine matrix crystals over the sample surface (Figure IA). Following data acquisition (Figure IB), MS images are constructed by depicting single ions (producing ion images) or by using statistical methods to combine multiple ions in a model to reveal a signature of key molecular changes within the tissue (producing classification images) [100] (Figure IC). The generated 'MS images' represent the spatial intensity distribution of certain *m/z* signals, which can be viewed as an intensity or pseudo-color heat map. The MS image can be merged with additional *m/z* values as well as superimposed onto the sample optical image. For accurate MSI analysis, a proper data-processing pipeline, including smoothing, baseline correction, normalization, background subtraction, and spectral recalibration, is required to eliminate the chemical and instrumental noises in MSI data [18].

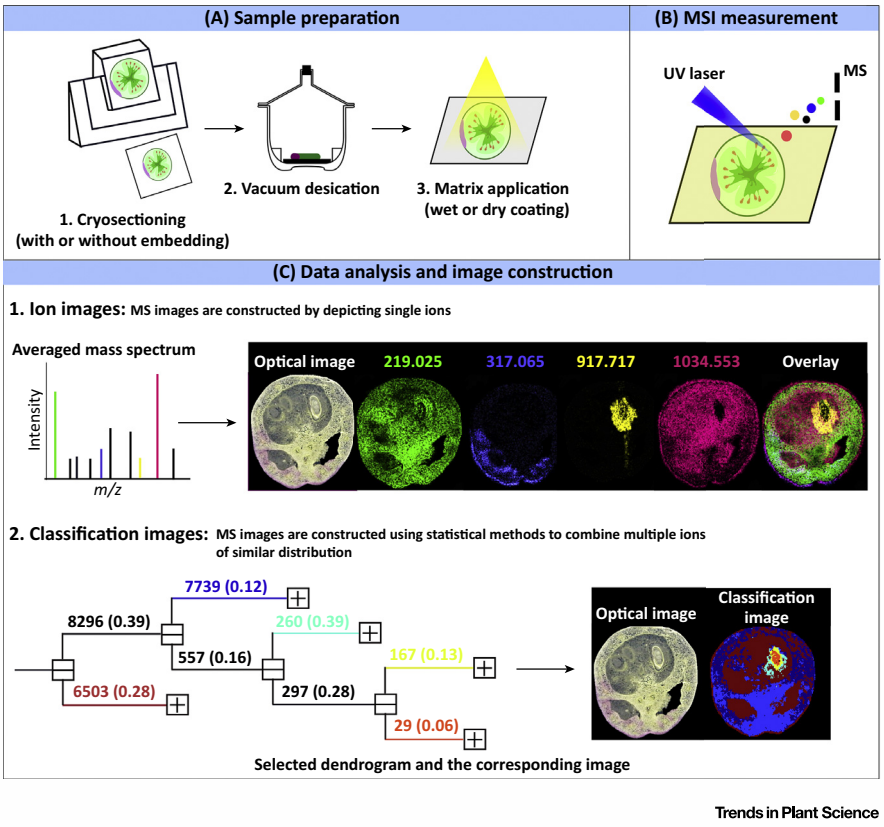

Figure I. Typical Workflow for Matrix-Assisted Laser Desorption Ionization (MALDI) Imaging.

Technical and Methodological Advances

The recent remarkable advancements in technology and methodological improvements have largely expanded the capacity of MSI. In this section, we highlight several notable concepts and innovations that will likely be of great benefit for plant biology research.

Mass Spectrometry Imaging at the Cellular Level

To fully understand the cellular specificity and functions of different cells, it is necessary to measure molecular signatures with single cell resolution [24]. High spatial resolution MSI requires a smaller region of sample tissue for each individual pixel. However, the reduced sampling

volume is accompanied by reduced ionization efficiency and sensitivity [25,26], which makes MSI at the single cell level challenging from a practical point of view.

SIMS is currently the predominant technique for single cell MSI owning to its submicron spatial resolution and excellent surface sensitivity [26]. It has been applied in various plants for the characterization of individual organelles, and most often localizes elements with a spatial resolution down to 1 μm [27–29]. Yet, it generally does not detect peptides, proteins, and most lipids [30]. MALDI is complementary to SIMS for mapping intact molecules, but its spatial resolution is typically limited to 20–100 μm [31,32]. Recent technical advances have enabled MALDI imaging with single cell resolution capability. A high-resolution atmospheric-pressure MALDI source has been developed for MSI of various plant tissues at a 5–10 μm spatial resolution [33,34]. Configuration of the laser in transmission geometry has been applied to achieve high spatial resolution MALDI imaging, as demonstrated by mapping the distribution of lipids and peptides in mammalian cells with 1 μm spatial resolution [35]. Additionally, incorporating the modified laser optics into a commercial MALDI instrument has improved the laser spot size from approximately 50 μm to approximately 9 μm, allowing MALDI imaging of a maize leaf at 5 μm spatial resolution with an oversampling method [25]. Oversampling involves the complete ablation of the MALDI matrix at each pixel and moving the sample target at a step size less than the laser beam size [36,37], hence enabling spatial resolutions smaller than the laser beam size. Apart from the beam size, the matrix crystal size is another important factor that limits MALDI imaging at the cellular level. Sublimation is the most common matrix coating approach for single cell MALDI imaging because it minimizes the delocalization of endogenous molecules and allows homogeneous matrix deposition with fine crystal size (<1 μm), as shown in the example of MALDI imaging of arabidopsis (*Arabidopsis thaliana*) at <10 μm spatial resolution [38]. Matrix-free laser desorption ionization (LDI) completely bypasses the limitation of matrix crystal size, allowing cellular imaging of most UV-absorbing analytes, such as anthocyanins and other related plant pigments [39,40].

3D Mass Spectrometry Imaging

Since biology is by and large a 3D phenomenon, it is not surprising that 3D MSI is emerging as a new frontier [41,42]. 3D MSI is currently carried out with two major approaches, serial section-based imaging and depth profiling. Serial section-based imaging is the most common approach, where serial tissue sections are collected and imaged individually with 2D MSI approaches. The 2D images are then used to reconstruct a 3D image [43,44]. This method is applicable to all MSI approaches. By contrast, the depth-profiling approach creates 3D images with a single tissue section by sputtering away several surface layers of the section to provide a submicrometer-depth resolution [42]. This method is only suitable for MSI approaches with depth-profiling capability, such as SIMS [45,46] and laser ablation electrospray ionization (LAESI) [47]. Using 3D LAESI imaging, a fungicide residue, imazalil, was localized on citrus fruit. The 3D image revealed that imazalil was present not only on the fruit skin surface, but also 400 μm below the skin [47], indicating that LAESI is a potentially simple and fast tool to determine agrochemical residues and/or contaminates in food. Given that LAESI does not require a very flat sample surface [47], it also allows for another 3D MSI mode, 3D surface imaging, where the imaging is performed over nonflat surfaces with 3D coordinates preserved for each data point [42].

Quantitative Mass Spectrometry Imaging

Quantitative MSI is intrinsically difficult because the MS signal is strongly affected by the local tissue chemical and morphological environment [48–51], known as ion suppression effects. For this reason, an internal standard (IS) is used in targeted quantitative MSI to compensate for the ion suppression effects and calibrate the raw ion intensities [50]. When the sample tissue is fairly morphologically homogeneous, quantitative MSI can be achieved by creating an on-tissue calibration curve [52]. A more general approach is to uniformly incorporate IS into the tissue, preferably an isotopically labeled IS since it has the identical extraction and ionization efficiency

as the target analyte [49]. In this case, IS can be added atop or beneath tissue sections with microspotting or spray-coating approaches [53]. The major limitation of IS-based quantitative MSI is that it requires targeted analysis because it is only applicable to a small fraction of ions observed in the spectrum [50]. In this aspect, IS-free quantitative MSI could have a significant advantage. The most common IS-free approach is to quantify analytes in the adjacent tissue sections by independent quantitative methods, such as LC-MS [54]; yet, this approach requires tedious sample extraction and analysis steps. Computational approaches are also being used to achieve IS-free quantitative MSI. For instance, a tissue- and analyte-specific normalization factor named 'tissue extinction coefficient' has been proposed to account for the ion suppression effect [55].

Multimodal Imaging

Each imaging technique has its own advantages and constraints [56]. For instance, MSI can generate rich chemical information, but the spatial resolution is still coarse; the classical imaging techniques, such as immunohistochemistry and magnetic resonance imaging (MRI), usually provide high structural resolution, but the chemical information is limited [5,57]. Combining MSI with other imaging modalities is becoming a topic of interest to obtain more detailed molecular and structural information, as shown by several selected examples detailed in Figure 2.

Apart from the combination of different MSI modalities for extra chemical and/or high spatial information, such as MALDI with DESI, and MALDI with SIMS [58], co-registration of

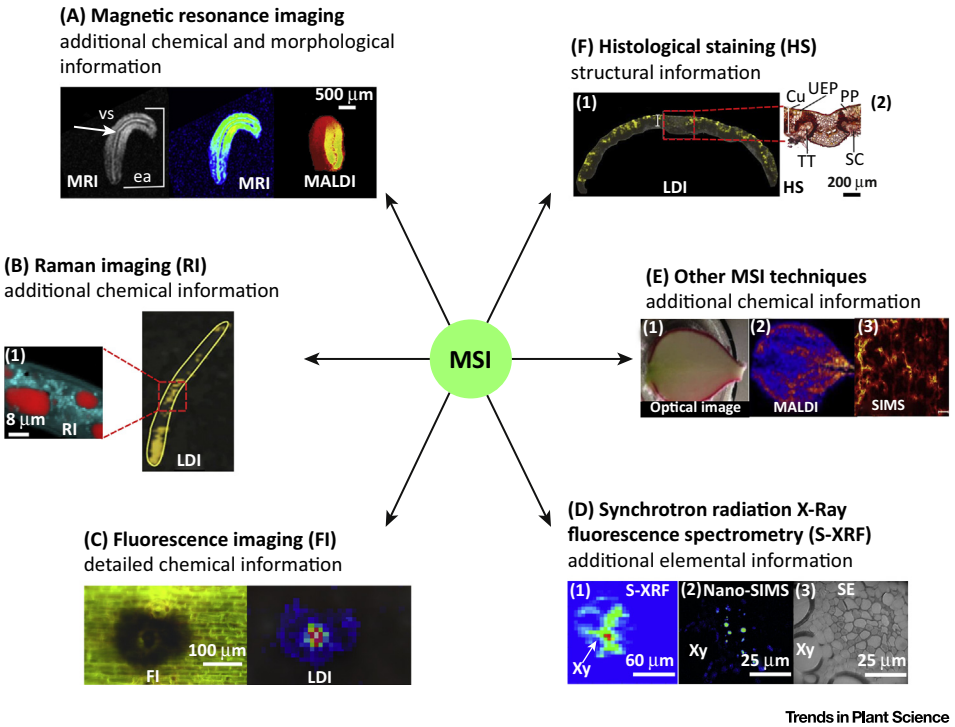

Figure 2. Selected Examples of Multimodal Mass spectrometry imaging (MSI) in Plant Research. (A) Matrix-assisted laser desorption ionization (MALDI) and magnetic resonance imaging (MRI) of lipids in *Camelina sativa* seed. (B) Laser desorption ionization (LDI) and Raman imaging of yellow droplets in nematodes. (C) LDI and fluorescent imaging of hydroxyanigorufone in red stomata and epidermis tissue of *Musa acuminata* ssp. *zebrine* cv. 'Rowe Red'. (D) Nano-secondary ion mass spectrometry (SIMS) and synchrotron X-ray fluorescence imaging of arsenic (As) in a leaf sheath of rice. (E) MALDI and SIMS imaging of choline in in radish bulb. (F) LDI imaging of flavonoid vicenin-2 in the transverse leaf sections of *Leucopogon ericoides*. The section was stained with Sudan for histological analysis. Adapted, with permission, from [59] (A), [60] (B), [97] (C), [98] (D), [58] (E), and [99] (F). Abbreviations: Cu, cuticle; EA, embryonic axis; PP, photosynthetic parenchyma; SC, stomatic crypt; SE, secondary electron image; TT, tector trichome; UEP, upper epidermis; VS, vascular system; Xy, xylem.

microscopic or histological image with MSI images is the most straightforward approach to gain more in-depth structural information and to aid data interpretation [4]. In addition, MRI has been coupled with MSI to visualize the detailed internal structure and distribution of some molecules. For instance, it has been coupled with MALDI imaging to map the lipids distribution in *Camelina sativa* seeds (Figure 2A) [59]. Owing to the capability of obtaining 3D anatomic structure in a non-invasive manner, there is interest in correlating MRI with 3D MSI. Raman spectroscopy imaging has also been combined with MSI to gain extra chemical information. An interesting example was reported in a study related to a banana–nematode interaction [60]. In this study, LDI-MSI was used to image a nematode-infected root of a resistant banana cultivar. The MS image revealed that the phytoalexin anigorufone accumulated in the nematode-induced root lesions, which could lead to the immobilization and eventual death of the nematodes. Further LDI-MSI analysis on the nematodes exposed to high concentrations of anigorufone showed that it was ingested and stored in yellow droplets in the nematode body. From a biochemical point of view, because anigorufone is non-water soluble, it should converge with lipids after being taken up. If those yellow droplets are rich in lipids, confidence in the identification of anigorufone detected in the LDI image would have been substantial. However, since LDI is incapable of imaging non-UV absorbing molecules, such as lipids, the authors used Raman microspectroscopy as a complementary tool to image the yellow droplets and the results showed that lipids were the major component of the yellow droplet (Figure 2B).

Application of Mass Spectrometry Imaging in Plant Sciences

Plant Physiology and Development

MSI was initially applied to visualize the distribution of molecules during plant growth, development, and reproduction [5,54,61–67]. A recent study focused on the spatiotemporal formation and deposition of lignan and cyanogenic glucoside in flax (*Linum usitatissimum*) capsules and seeds during development [63]. The MALDI imaging results showed that the lignans, secoisolariciresinol diglucoside (SDG) and 6a-hydroxymethylglutaric acid (HMG)-SDG, were detectable only during the early seed coat development stages and, during seed coat maturation, SDG derivatives were converted into higher-molecular-weight phenolics. By contrast, cyanogenic glucosides (the monoglucosides linamarin and lotaustralin) were localized throughout the flax capsule, while the diglucosides linustatin and neolinustatin accumulated only in endosperm and embryo tissues (Figure 3A).

A multimodal MSI approach has been used to study the nitrogen cycle in radish plants (*Raphanus sativus*). Radish plants were grown in a hydroponic system with N^{15}-labeled KNO_3 being the only nitrogen source. The harvested radishes were fermented in water to create a radish 'tea', which was used as the nitrogen source for the second-generation radish to grow. The MALDI imaging results showed that approximately 50% of nitrogen from the dead radish plants was assimilated into amino acids in the second-generation radish plants, and the amino acids were distributed heterogeneously in radish bulb; for instance, choline was abundant near to the skin of the bulbs. High-resolution SIMS imaging was further applied to map the detailed distribution of choline in the center area of the radish bulb (Figure 2E) [58]. As shown in this example, the use of N^{15}-labeled KNO_3 enabled the spatial tracking of the absorption, translocation, and assimilation of nitrogen in radish with MSI, which highlights the potential of using stable isotope labeling in MSI to capture dynamic metabolic information and visualize how individual pathways or metabolic networks are interconnected.

Functional Genomics

MSI is an excellent tool to discover changes in mutants or any genetically modified plants through comparisons with control samples, and, thus, is most valuable in gene discovery studies. In a proof-of-principle study, the distribution of flavonoids in wild-type and the *tt7* mutant arabidopsis flowers was investigated (Figure 3B) [68]. The MALDI imaging results

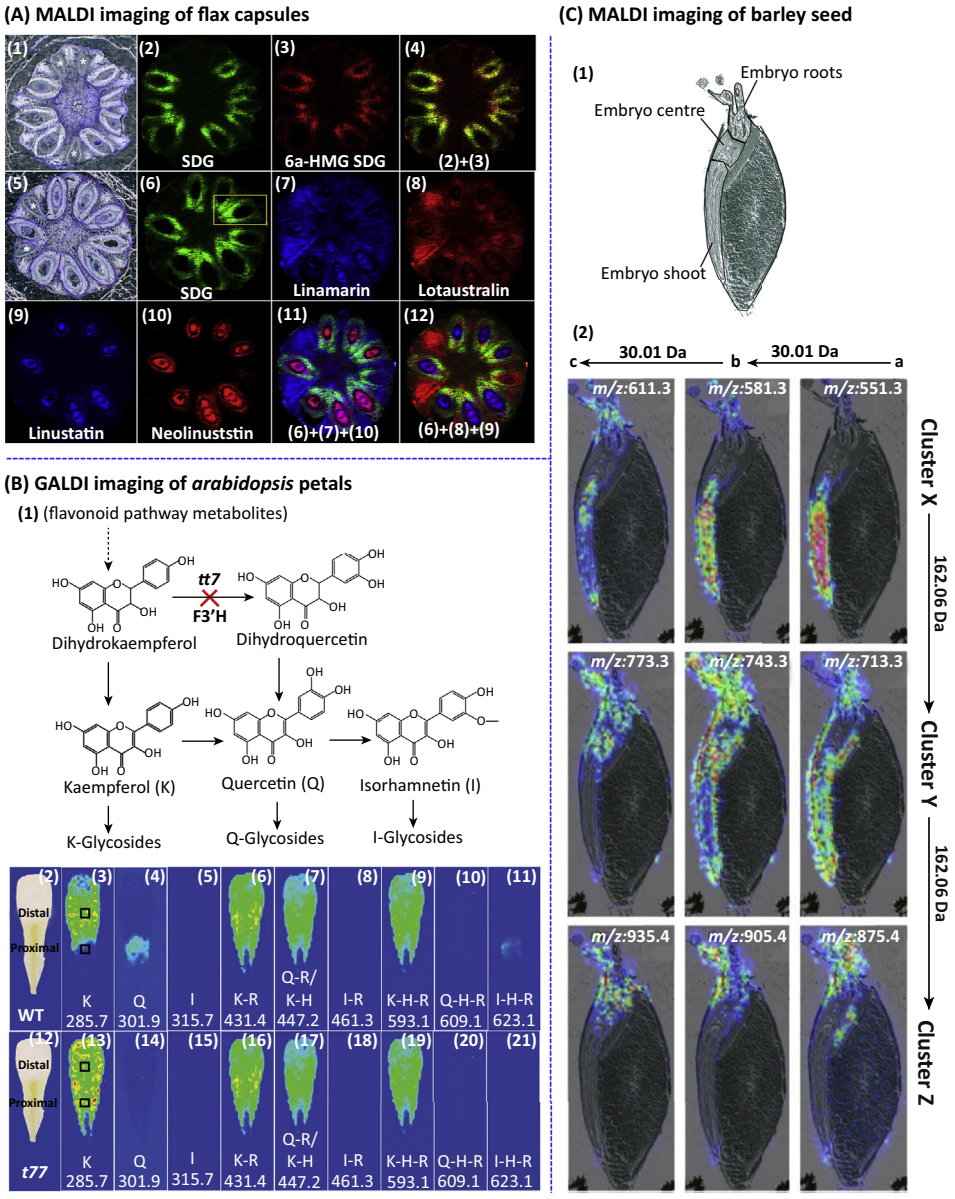

Figure 3. Application of Mass Spectrometry Imaging (MSI) in Plant Research. (A) Matrix-Assisted Laser Desorption Ionization (MALDI)-images of flax capsules. (1) Optical image of a cross-section of a capsule (6 DAF: day after flowing) stained with toluidine blue O. (2,3) MALDI images of secoisolariciresinol diglucoside (SDG) (2) and 6a-hydroxymethylglutaric acid (HMG)-SDG (3) in the 6 DAF flax capsule. (4) Merged MALDI images of (2) and (3). (5) Optical image of a cross-section of capsule (7 DAF) stained with toluidine blue O. (6–10) MALDI image of SDG (6), linamarin (7), lotaustralin (8), linustatin (9), and neolinustatin (10) in the 7 DAF flax capsule. (11) Merged MALDI images of (6), (7), and (10). (12) Merged MALDI images of (6), (8), and (9). * in (1) and (5) indicates seeds that did not develop. (B) GALDI imaging of arabidopsis petals. (1) Partial representation of the flavonoid biosynthetic pathway in *Arabidopsis*. (2,12) Optical images of wild type (2) and *tt7* mutant (12). (3–11,13–21) The arabidopsis petals showing distributions of the flavonoids kaempferol (K), quercetin (Q), and isorhamnetin (I), along with their rhamnose (R) and hexose-rhamnose (H-R) glycosides in both wild-type (3-11) and *tt7* mutant (13-21) petals. (C) MALDI imaging of barley seed. (1) Optical image of a longitudinal section of a 3-day germinated barley seed. (2) MALDI images of annotated cluster X, Y, and Z compounds. Compound distribution maps were organized according to the mass distances with +30.02 Da in lines (hordatines a, b, and c) and +162.14 Da in columns (X, Y, and Z for glycosylation states). Adapted from [63] (A), [68] (B), and [71] (C).

showed that kaempferol localized at the distal region, and quercetin and isorhamnetin at the proximal end of wild-type petals. By contrast, neither quercetin nor isorhamnetin was detected in the mutant flowers since the mutation in the *TT7* gene blocked the conversion of dihydrokaempferol to dihydroquercetin, and, therefore, the formation of the downstream quercetin and isorhamnetin flavonols. As a consequence, this mutation leads to the accumulation of kaempferol in the whole petal. In particular, the total amount of flavonols in the proximal region of petals in the wild type were nearly equivalent to the amount of kaempferol in the mutant, suggesting that the expression of the *TT7* gene is localized to the proximal part of the petal, while the other genes in the upstream pathway are uniformly expressed in the petal.

Novel Metabolites and Biomarkers Discovery

A molecule that is confined to a relatively small area would be detected by MSI, but not necessarily by LC-MS or GC-MS of a whole-sample homogenate because it would be diluted in the complete sample [30]. This highlights the potential of MSI to assist the discovery of novel metabolites or biomarkers. A new β-carboline alkaloid, 6-hydroxymetatacarboline D, from the fruiting bodies of mushrooms (*Mycena metata*) has been identified, and MALDI imaging showed that it was exclusively located on the top surface of the fruiting body [69]. Another similar example was the discovery of noncyclic peptides, named 'acyclotides', from *Petunia x hybrida* (petunia), which were found to be abundant in vascular tissues [70]. Colocalized metabolites might be derivatives of the same metabolic pathway. Following this concept, 19 unknown hordatine derivatives and four novel precursors were identified in barley seeds according to their colocalization with the pre-identified hordatine by the use of MALDI imaging (Figure 3C) [71].

Furthermore, knowing the compound localization is valuable for the optimization of compound-specific extraction [72]. For instance, the distribution of triacylglycerol (TAG) distribution in avocado fruit has been mapped using MALDI imaging. According to the distribution pattern, the central mesocarp region was selected to extract lipid droplets. After proteome and transcript analysis of the extracted lipid droplets, two new lipid droplet-associated proteins were identified [73].

Plant–Environment Interactions

Production of many plant metabolites is induced or repressed in response to environmental cues. MSI provides a unique tool to track the spatiotemporal response upon exposure to biotic and/or abiotic stresses, including the plant–UV light response [74], root–soil interactions [75], plant–insect and/or pathogen crosstalk [60,76–83], and symbiotic nitrogen fixation [84–86].

In a relatively early example, the distribution of glucosinolates was mapped in arabidopsis leaves using MALDI imaging. The major glucosinolates were found to be more abundant in the mid-vein and the periphery of the leaf than in the inner lamina. This distribution was found to be correlated with the feeding pattern of the cotton bollworm (*Helicoverpa armigera*), which fed almost exclusively on the inner lamina [87]. By spotting known amounts of glucosinolates on the leaf surface, the same research group was able to quantify the total amount of glucosinolates in the arabidopsis leaf surface. The concentrations of glucosinolates on the leaf surfaces were found to be sufficient to attract the specialist feeding lepidopterans *Plutella xylostella* and *Pieris rapae* for oviposition [52]. Both studies suggested that the non-uniform distribution of glucosinolates in arabidopsis directly protects the most vulnerable or valuable regions from herbivory by accumulating glucosinolates to deter generalist insect herbivores or attract specialist herbivores to choose the plants for oviposition.

Concluding Remarks and Future Perspectives

MSI has evolved as a powerful tool to characterize the chemically, spatially, and temporally complex plant systems. Issues such as limited molecular coverage, difficulty in molecule annotation, and the challenges in *in vivo* MSI are the tasks to be addressed in the near future.

Outstanding Questions

How can we simplify and automate sample preparation for more accurate and reproducible MSI?

How can MSI be combined with widely used molecular imaging techniques in plant research, such as GFP imaging and fluorescence *in situ* hybridization?

Can MSI be used for direct monitoring of gene expression and enzyme activity?

How can we achieve non-invasive and time-resolved *in vivo* MSI?

What can be done to improve confidence in molecule identification and reliable quantitative MSI?

Continual improvements in instrumentation, sample preparation, analytical strategy, and data analysis are expected to allow more effective and widespread application of MSI in plant research (see Outstanding Questions).

Instrumental improvements in spatial resolution and speed are required to enable optimal spatial analysis in less time. Nondestructive MSI ion sources are needed for *in vivo* and time-resolved MSI analysis on the same tissue sample. Further development of sample preparation methods holds much promise to compensate ion suppression effects, enhance molecular coverage, and improve quantitative MSI.

Molecular coverage and metabolite annotation remain considerable challenges in MSI experiments. In LC-MS or GC-MS analyses, metabolite identification relies to a large extent on the combination of retention time and MS data, while the lack of chromatographic separation in MSI not only results in limited molecular coverage, but also makes metabolite identification more complex [88]. Novel analytical strategies are being developed to improve molecular coverage and metabolite identification. For example, combining MSI with other imaging modalities significantly increases the validity of MSI data [14]; coupling **ion-mobility spectrometry** with MSI enables wider ion coverage, allowing structure determination of different isomeric and isobaric peaks [89]; and **reactive MSI**, such as reactive MALDI [90] and reactive DESI imaging [91,92], has been developed to detect compounds that were previously intractable.

Data analysis is another significant bottleneck in MSI. A typical MSI data set includes thousands of mass spectra, each of which comprise thousands of intensity values; therefore, a single data set can easily approach gigabytes [93]. The size of the data sets can increase dramatically when using high spatial resolution and high mass resolution MSI techniques or using 3D MSI [94,95]. Runtime and memory-efficient computational methods are required to overcome these issues. Further development of MSI-specific statistical methods that take into account the spatial information within the MSI data set are needed to efficiently discover the co-occurring metabolites and significant differences in regions of tissue [4]. In addition, the multiplicity of data formats generated by various mass spectrometers from different manufacturers hampers MSI data storage and management [93]. Several open standard formats have been proposed to solve this problem, such as imzML [93] and the OpenMSI file format [96]. In particular, OpenMS[i] is a web-based platform for MSI data management, analysis, and visualization, and the use of the OpenMSI file format has shown to provide an over 2000-fold improvement for image-access operations [96].

As MSI develops, this exciting technology will no doubt bring valuable insights that will 'change the picture' in many areas of plant research.

Acknowledgments

We thank the Tom and Sondra Rykoff Family Foundation Research and the Israeli Centers of Research Excellence (i-CORE) program on Plant Adaptation to Changing Environment for supporting the A.A. lab activity. A.A. is the incumbent of the Peter J. Cohn Professorial Chair.

Resources

[i] https://openmsi.nersc.gov

References

1. Wood, P.L. (2014) Mass spectrometry strategies for clinical metabolomics and lipidomics in psychiatry, neurology, and neuro-oncology. *Neuropsychopharmacology* 39, 24–33
2. Moussaieff, A. *et al.* (2013) High-resolution metabolic mapping of cell types in plant roots. *Proc. Natl. Acad. Sci. U.S.A.* 110, E1232–E1241
3. Goldberg, R.B. (1988) Plants: novel developmental processes. *Science* 240, 1460–1467
4. Boughton, B.A. *et al.* (2015) Mass spectrometry imaging for plant biology: a review. *Phytochem. Rev.* 1–44

5. Bhandari, D.R. *et al.* (2015) High resolution mass spectrometry imaging of plant tissues: towards a plant metabolite atlas. *Analyst* 140, 7696–7709
6. Kueger, S. *et al.* (2012) High-resolution plant metabolomics: from mass spectral features to metabolites and from whole-cell analysis to subcellular metabolite distributions. *Plant J.* 70, 39–50
7. Carter, A.D. *et al.* (2013) The use of fluorescence-activated cell sorting in studying plant development and environmental responses. *Int. J. Dev. Biol.* 57, 545–552
8. Sumner, L.W. *et al.* (2015) Modern plant metabolomics: advanced natural product gene discoveries, improved technologies, and future prospects. *Nat. Pro. Rep.* 32, 212–229
9. Rogers, E.D. *et al.* (2012) Cell type-specific transcriptional profiling: implications for metabolite profiling. *Plant J.* 70, 5–17
10. Kiss, A. *et al.* (2013) Cluster secondary ion mass spectrometry microscope mode mass spectrometry imaging. *Rapid Commun. Mass Spectrom.* 27, 2745–2750
11. Griffiths, W.J. and Wang, Y. (2009) Mass spectrometry: from proteomics to metabolomics and lipidomics. *Chem. Soc. Rev.* 38, 1882–1896
12. Jungmann, J.H. and Heeren, R.M. (2012) Emerging technologies in mass spectrometry imaging. *J. Proteomics* 75, 5077–5092
13. Goodwin, R.J. *et al.* (2008) Protein and peptides in pictures: imaging with MALDI mass spectrometry. *Proteomics* 8, 3785–3800
14. Spengler, B. (2014) Mass spectrometry imaging of biomolecular information. *Anal. Chem.* 87, 64–82
15. Kiss, A. *et al.* (2013) Microscope mode secondary ion mass spectrometry imaging with a Timepix detector. *Rev. Sci. Instrum.* 84, 013704
16. Amstalden van Hove, E.R. *et al.* (2010) A concise review of mass spectrometry imaging. *J. Chromatogr. A* 1217, 3946–3954
17. Svatos, A. (2010) Mass spectrometric imaging of small molecules. *Trends Biotechnol.* 28, 425–434
18. Heyman, H.M. and Dubery, I.A. (2015) The potential of mass spectrometry imaging in plant metabolomics: a review. *Phytochem. Rev.* 15, 297–316
19. Bjarnholt, N. *et al.* (2014) Mass spectrometry imaging of plant metabolites-principles and possibilities. *Nat. Prod. Rep.* 31, 818–837
20. Li, B. *et al.* (2015) Analytical capabilities of mass spectrometry imaging and its potential applications in food science. *Trends Food Sci. Tech.* 47, 50–63
21. Bartels, B. and Svatoš, A. (2015) Spatially resolved in vivo plant metabolomics by laser ablation-based mass spectrometry imaging (MSI) techniques: LDI-MSI and LAESI. *Front. Plant Sci.* 6, 471
22. Sturtevant, D. *et al.* (2016) Matrix assisted laser desorption/ionization-mass spectrometry imaging (MALDI-MSI) for direct visualization of plant metabolites in situ. *Curr. Opin. Biotechnol.* 37, 53–60
23. Dong, Y. *et al.* (2016) Sample preparation for mass spectrometry imaging of plant tissues: a review. *Front. Plant Sci.* 7, 60
24. Wang, D. and Bodovitz, S. (2010) Single cell analysis: the new frontier in 'omics'. *Trends Biotechnol.* 28, 281–290
25. Korte, A.R. *et al.* (2015) Subcellular-level resolution MALDI-MS imaging of maize leaf metabolites by MALDI-linear ion trap-Orbitrap mass spectrometer. *Anal. Bioanal. Chem.* 407, 2301–2309
26. Passarelli, M.K. and Ewing, A.G. (2013) Single-cell imaging mass spectrometry. *Curr. Opin. Chem. Biol.* 17, 854–859
27. Bougoure, J. *et al.* (2014) High-resolution secondary ion mass spectrometry analysis of carbon dynamics in mycorrhizas formed by an obligately myco-heterotrophic orchid. *Plant Cell Environ.* 37, 1223–1230
28. Kyriacou, B. *et al.* (2014) Localization of iron in rice grain using synchrotron X-ray fluorescence microscopy and high resolution secondary ion mass spectrometry. *J. Cereal Sci.* 59, 173–180
29. Saito, K. *et al.* (2014) Aluminum localization in the cell walls of the mature xylem of maple tree detected by elemental imaging using time-of-flight secondary ion mass spectrometry (TOF-SIMS). *Holzforschung* 68, 85–92
30. Boggio, K.J. *et al.* (2011) Recent advances in single-cell MALDI mass spectrometry imaging and potential clinical impact. *Expert Rev. Proteomics* 8, 591–604
31. Römpp, A. and Spengler, B. (2013) Mass spectrometry imaging with high resolution in mass and space. *Histochem. Cell Biol.* 139, 759–783
32. Schober, Y. *et al.* (2012) Single cell matrix-assisted laser desorption/ionization mass spectrometry imaging. *Anal. Chem.* 84, 6293–6297
33. Li, B. *et al.* (2014) Natural products in licorice (*Glycyrrhiza glabra*) rhizome imaged at the cellular level by atmospheric pressure matrix-assisted laser desorption/Ionization tandem mass spectrometry imaging. *Plant J.* 80, 161–171
34. Römpp, A. *et al.* (2010) Histology by mass spectrometry: label-free tissue characterization obtained from high-accuracy bioanalytical imaging. *Angew. Chem. Int. Ed.* 49, 3834–3838
35. Zavalin, A. *et al.* (2012) Direct imaging of single cells and tissue at sub-cellular spatial resolution using transmission geometry MALDI MS. *J. Mass Spectrom.* 47, 1473–1481
36. Jurchen, J.C. *et al.* (2005) MALDI-MS imaging of features smaller than the size of the laser beam. *J. Am. Soc. Mass Spectrom.* 16, 1654–1659
37. Nazari, M. and Muddiman, D.C. (2014) Cellular-level mass spectrometry imaging using infrared matrix-assisted laser desorption electrospray ionization (IR-MALDESI) by oversampling. *Anal. Bioanal. Chem.* 407, 2265–2271
38. Takahashi, K. *et al.* (2015) Development and application of a high-resolution imaging mass spectrometer for the study of plant tissues. *Plant Cell Physiol.* 56, 1329–1338
39. Holscher, D. *et al.* (2009) Matrix-free UV-laser desorption/ionization (LDI) mass spectrometric imaging at the single-cell level: distribution of secondary metabolites of *Arabidopsis thaliana* and *Hypericum* species. *Plant J.* 60, 907–918
40. Jaschinski, T. *et al.* (2014) Matrix-free single-cell LDI-MS investigations of the diatoms *Coscinodiscus granii* and *Thalassiosira pseudonana*. *J. Mass Spectrom.* 49, 136–144
41. Seeley, E.H. and Caprioli, R.M. (2012) 3D imaging by mass spectrometry: a new frontier. *Anal. Chem.* 84, 2105–2110
42. Palmer, A.D. and Alexandrov, T. (2015) Serial 3D imaging mass spectrometry at its tipping point. *Anal. Chem.* 87, 4055–4062
43. Oetjen, J. *et al.* (2013) MRI-compatible pipeline for three-dimensional MALDI imaging mass spectrometry using PAXgene fixation. *J. Proteomics* 90, 52–60
44. Lanekoff, I. *et al.* (2015) Three-dimensional imaging of lipids and metabolites in tissues by nanospray desorption electrospray ionization mass spectrometry. *Anal. Bioanal. Chem.* 407, 2063–2071
45. Körsgen, M. *et al.* (2015) 3D ToF-SIMS analysis of peptide incorporation into MALDI matrix crystals with sub-micrometer resolution. *J. Am. Soc. Mass Spectrom.* 27, 277–284
46. Bailey, J. *et al.* (2015) 3D ToF-SIMS Imaging of polymer multilayer films using argon cluster sputter depth profiling. *ACS Appl. Mater. Interfaces* 7, 2654–2659
47. Nielen, M.W. and van Beek, T.A. (2014) Macroscopic and microscopic spatially-resolved analysis of food contaminants and constituents using laser-ablation electrospray ionization mass spectrometry imaging. *Anal. Bioanal. Chem.* 406, 6805–6815
48. Tomlinson, L. *et al.* (2014) Using a single, high mass resolution mass spectrometry platform to investigate ion suppression effects observed during tissue imaging. *Rapid Commun. Mass Spectrom.* 28, 995–1003
49. Lietz, C.B. *et al.* (2013) Qualitative and quantitative mass spectrometry imaging of drugs and metabolites. *Adv. Drug Deliv. Rev.* 65, 1074–1085
50. Ellis, S.R. *et al.* (2014) A critical evaluation of the current state-of-the-art in quantitative imaging mass spectrometry. *Anal. Bioanal. Chem.* 406, 1275–1289
51. Dong, Y. *et al.* (2016) Impact of tissue surface properties on the desorption electrospray ionization imaging of organic acids in grapevine stem. *Rapid Commun. Mass Spectrom.* 30, 711–718
52. Shroff, R. *et al.* (2015) Quantification of plant surface metabolites by matrix-assisted laser desorption-ionization mass spectrometry

imaging: glucosinolates on *Arabidopsis thaliana* leaves. *Plant J.* 81, 961–972

53. Pirman, D.A. *et al.* (2012) Quantitative MALDI tandem mass spectrometric imaging of cocaine from brain tissue with a deuterated internal standard. *Anal. Chem.* 85, 1081–1089
54. Li, B. *et al.* (2013) Visualizing metabolite distribution and enzymatic conversion in plant tissues by desorption electrospray ionization mass spectrometry imaging. *Plant J.* 74, 1059–1071
55. Hamm, G. *et al.* (2012) Quantitative mass spectrometry imaging of propranolol and olanzapine using tissue extinction calculation as normalization factor. *J. Proteomics* 75, 4952–4961
56. Van de Plas, R. *et al.* (2015) Image fusion of mass spectrometry and microscopy: a multimodality paradigm for molecular tissue mapping. *Nat. Methods* 12, 366–372
57. Feenstra, A.D. *et al.* (2015) Multi-matrix, dual polarity, tandem mass spectrometry imaging strategy applied to a germinated maize seed: toward mass spectrometry imaging of an untargeted metabolome. *Analyst* 140, 7293–7304
58. Seaman, C. *et al.* (2014) Afterlife Experiment": use of MALDI-MS and SIMS imaging for the study of the nitrogen cycle within plants. *Anal. Chem.* 86, 10071–10077
59. Horn, P.J. *et al.* (2013) Imaging heterogeneity of membrane and storage lipids in transgenic *Camelina sativa* seeds with altered fatty acid profiles. *Plant J.* 76, 138–150
60. Hölscher, D. *et al.* (2014) Phenalenone-type phytoalexins mediate resistance of banana plants (*Musa* spp.) to the burrowing nematode *Radopholus similis*. *Proc. Natl. Acad Sci. U.S.A.* 111, 105–110
61. Veličković, D. *et al.* (2014) New insights into the structural and spatial variability of cell-wall polysaccharides during wheat grain development, as revealed through MALDI mass spectrometry imaging. *J. Exp. Bot.* 65, 2079–2091
62. Peukert, M. *et al.* (2014) Spatio-temporal dynamics of fructan metabolism in developing barley grains. *Plant Cell* 26, 3728–3744
63. Dalisay, D.S. *et al.* (2015) Dirigent protein-mediated lignan and cyanogenic glucoside formation in flax seed: integrated omics and MALDI mass spectrometry imaging. *J. Nat. Prod.* 78, 1231–1242
64. Gerbig, S. *et al.* (2015) Spatially resolved investigation of systemic and contact pesticides in plant material by desorption electrospray ionization mass spectrometry imaging (DESI-MSI). *Anal. Bioanal. Chem.* 407, 7379–7389
65. Lingott, J. *et al.* (2015) Gadolinium-uptake by aquatic and terrestrial organisms: distribution determined by laser ablation inductively coupled plasma mass spectrometry. *Environ. Sci. Processes Impacts* 18, 200–207
66. Garrett, R. *et al.* (2016) Revealing the spatial distribution of chlorogenic acids and sucrose across coffee bean endosperm by desorption electrospray ionization-mass spectrometry imaging. *LWT-Food Sci. Technol.* 65, 711–717
67. Yamamoto, K. *et al.* (2016) Cell-specific localization of alkaloids in *Catharanthus roseus* stem tissue measured with imaging MS and single-cell MS. *Proc. Natl. Acad. Sci. U.S.A.* http://dx.doi.org/10.1073/pnas.1521959113
68. Korte, A.R. *et al.* (2012) Mass spectrometric imaging as a high-spatial resolution tool for functional genomics: tissue-specific gene expression of TT7 inferred from heterogeneous distribution of metabolites in *Arabidopsis* flowers. *Anal. Methods* 4, 474–481
69. Jaeger, R.J. *et al.* (2013) HR-MALDI-MS imaging assisted screening of beta-Carboline alkaloids discovered from *Mycena metata*. *J. Nat. Prod.* 72, 127–134
70. Poth, A.G. *et al.* (2012) Cyclotides associate with leaf vasculature and are the products of a novel precursor in *Petunia* (Solanaceae). *J. Biol. Chem.* 287, 27033–27046
71. Gorzolka, K. *et al.* (2014) Detection and localization of novel hordatine-like compounds and glycosylated derivates of hordatines by imaging mass spectrometry of barley seeds. *Planta* 239, 1321–1335
72. Bai, H. *et al.* (2016) Localization of ginsenosides in *Panax* ginseng with different age by matrix-assisted laser-desorption/ionization time-of-flight mass spectrometry imaging. *J. Chromatogr. B.* 1026, 263–271
73. Horn, P.J. *et al.* (2013) Identification of a new class of lipid droplet-associated proteins in plants. *Plant Physiol.* 162, 1926–1936
74. Becker, L. *et al.* (2014) MALDI mass spectrometry imaging for the simultaneous location of resveratrol, pterostilbene and viniferins on grapevine leaves. *Molecules* 19, 10587–10600
75. Rudolph-Mohr, N. *et al.* (2015) Non-invasive imaging techniques to study O2 micro-patterns around pesticide treated lupine roots. *Geoderma* 239, 257–264
76. Ryffel, F. *et al.* (2015) Metabolic footprint of epiphytic bacteria on *Arabidopsis thaliana* leaves. *The ISME Journal* 10, 632–643
77. Klein, A.T. *et al.* (2015) Investigation of the chemical interface in the soybean-aphid and rice-bacteria interactions using MALDI-mass spectrometry imaging. *Anal. Chem.* 87, 5294–5301
78. Soares, M.S. *et al.* (2015) Quantification and localization of hesperidin and rutin in *Citrus sinensis* grafted on *C. limonia* after *Xylella fastidiosa* infection by HPLC-UV and MALDI imaging mass spectrometry. *Phytochemistry* 115, 161–170
79. Debois, D. *et al.* (2014) Spatiotemporal monitoring of the antibiome secreted by *Bacillus* biofilms on plant roots using MALDI mass spectrometry imaging. *Anal. Chem.* 86, 4431–4438
80. Tata, A. *et al.* (2014) Analysis of metabolic changes in plant pathosystems by imprint imaging DESI-MS. *J. Am. Soc. Mass Spectrom.* 26, 641–648
81. Etalo, D.W. *et al.* (2015) Spatially resolved plant metabolomics: some potentials and limitations of laser-ablation electrospray ionization mass spectrometry metabolite imaging. *Plant Physiol.* 169, 1424–1435
82. Wang, W-X. *et al.* (2015) Hexacyclopeptides secreted by an endophytic fungus *Fusarium solani* N06 act as crosstalk molecules in *Narcissus tazetta*. *App. Microbiol. Biotech.* 99, 7651–7662
83. Debois, D. *et al.* (2015) Plant polysaccharides initiate underground crosstalk with bacilli by inducing synthesis of the immunogenic lipopeptide surfactin. *Environ. Microbiol. Rep.* 7, 570–582
84. Ye, H. *et al.* (2013) MALDI mass spectrometry-assisted molecular imaging of metabolites during nitrogen fixation in the *Medicago truncatula-Sinorhizobium meliloti* symbiosis. *Plant J.* 75, 130–145
85. Gemperline, E. and Li, L. (2014) MALDI-mass spectrometric imaging for the investigation of metabolites in *Medicago truncatula* root nodules. *JoVE.* http://dx.doi.org/10.3791/51434
86. Gemperline, E. *et al.* (2015) Multifaceted investigation of metabolites during nitrogen fixation in *Medicago* via high resolution MALDI-MS imaging and ESI-MS. *J. Am Soc. Mass Spectrom.* 26, 149–158
87. Shroff, R. *et al.* (2008) Nonuniform distribution of glucosinolates in *Arabidopsis thaliana* leaves has important consequences for plant defense. *Proc. Natl. Acad. Sci. U.S.A.* 105, 6196–6201
88. Miura, D. *et al.* (2012) In situ metabolomic mass spectrometry imaging: recent advances and difficulties. *J. Proteomics* 75, 5052–5060
89. Li, H. *et al.* (2015) Ambient molecular imaging by laser ablation electrospray ionization mass spectrometry with ion mobility separation. *Int. J. Mass Spectrom.* 377, 681–689
90. Shariatgorji, M. *et al.* (2015) Pyrylium salts as reactive matrices for MALDI-MS imaging of biologically active primary amines. *J. Am. Soc. Mass Spectrom.* 26, 934–939
91. Lostun, D. *et al.* (2015) Reactive DESI-MS imaging of biological tissues with dicationic ion-pairing compounds. *Anal. Chem.* 87, 3286–3293
92. Rao, W. *et al.* (2015) High-resolution ambient MS imaging of negative ions in positive ion mode: using dicationic reagents with the single-probe. *J. Am. Soc. Mass Spectrom.* 27, 124–134
93. Robbe, M-F. *et al.* (2014) Software tools of the Computis European project to process mass spectrometry images. *Eur. J. Mass Spectrom.* 20, 351–360
94. Alexandrov, T. (2012) MALDI imaging mass spectrometry: statistical data analysis and current computational challenges. *BMC bioinformatics* 13 (Suppl. 16), S11

95. Fischer, C.R. *et al.* (2016) An accessible, scalable ecosystem for enabling and sharing diverse mass spectrometry imaging analyses. *Arch. Biochem. Biophys.* 589, 18–26
96. Rübel, O. *et al.* (2013) OpenMSI: a high-performance web-based platform for mass spectrometry imaging. *Anal. Chem.* 85, 10354–10361
97. Hölscher, D. *et al.* (2015) High resolution mass spectrometry imaging reveals the occurrence of phenylphenalenone-type compounds in red paracytic stomata and red epidermis tissue of *Musa acuminata* ssp. *zebrina* cv. 'Rowe Red'. *Phytochemistry* 116, 239–245
98. Moore, K.L. *et al.* (2014) Combined NanoSIMS and synchrotron X-ray fluorescence reveal distinct cellular and subcellular distribution patterns of trace elements in rice tissues. *New Phytol.* 201, 104–115
99. Silva, D.B. *et al.* (2014) Mass spectrometry of flavonoid vicenin-2, based sunlight barriers in *Lychnophora* species. *Sci. Rep.* 4, 4309
100. Schwamborn, K. and Caprioli, R.M. (2010) Molecular imaging by mass spectrometry-looking beyond classical histology. *Nat. Rev. Cancer* 10, 639–646